

# Contributions of Numerical Simulation in the Development of Pulse Tube Cryocoolers

C. Wang

Boston Cryogenics LLC  
Boston, MA 01719

## ABSTRACT

Numerical simulation is an effective tool to analyze the internal operating process of pulse tube (PT) cryocoolers, which has contributed to the innovation and improvement of PT cryocoolers. This paper reviews major contributions of numerical simulation, such as (1) revealing and confirming the concept of “gas piston” in the pulse tube; (2) analyzing the phase-shifting mechanism of an orifice PT cryocooler; (3) the invention of a double-inlet PT cryocooler and analyzing functions of the double-inlet; (4) discovering and analyzing “DC flow” effects in PT cryocoolers; (5) revealing unique features of 4 K regenerators and analyzing the enthalpy losses of 4 K regenerators for the intercept cooling; and (6) assisting inventions of new phase shifters for PT cryocoolers by analyzing their phase-shifting mechanism.

## INTRODUCTION

Developments of PT cryocoolers have gone through a few milestones in the past 58 years. The first basic PT cryocooler was invented in 1964 by Gifford and Longsworth [1]. It had then been buried for nearly two decades because of its poor cooling performance. The invention of an orifice PT cryocooler by Mikulin et al. in 1984 [2] ignited the worldwide development of PT cryocoolers.

The orifice PT cryocooler employs an orifice and gas reservoir to perform as a phase shifter for mass flow and pressure. It can operate as a traditional cryocooler such as GM, Stirling, and Solvay cryocooler.

The working mechanism of orifice PT cryocoolers is more complicated than traditional cryocoolers. There were many questions concerning the operation of the orifice PT cryocooler at the beginning.

Numerical simulation (also called nodal analysis, numerical analysis, or numerical modeling) of Stirling engines was pioneered by Finkelstein in 1975 [3]. D. Gedeon outlined the techniques of Stirling engine simulation in use at Sunpower of Athen, Ohio in 1978 [4]. The numerical simulation program was initially available for general use on a contract basis. Later on, the program was developed and named as “Sage” program, a commercial software program, which is widely used for PT cryocoolers.

The numerical simulation can effectively reveal the internal process of cryocoolers from engineering aspects. Numerical simulation of a PT cryocooler was first started at Xian Jiaotong

University. Owing to the Numerical Heat Transfer Class offered at Xian Jiaotong University in the late 1980s [5], students in the cryogenic group led by Prof. Peiyi Wu had opportunities to take the class and grasp the skills of numerical simulation. Three researchers of PT cryocooler, who graduated from the cryogenics group at Xian Jiaotong University, Dr. Shaowei Zhu, Dr. Chao Wang, and Dr. Mingyao Xu, have performed substantial numerical simulations during their development and benefited from the results of numerical analysis.

Numerical simulation reveals the internal working process, which helps to understand the operation of the cryocooler, guides the system design, and contributes to the innovation of PT cryocoolers. This paper reviews the major contributions of the numerical simulations for the PT cryocoolers.

## NUMERICAL SIMULATION

Numerical simulation is completed by defining a physical model with boundary conditions; giving governing equations, performing domain discretization and equation discretization; solving energy equations, and writing a computer program to simulate the cryocooler operation.

The governing equations for simulation are given as follows:

Energy equation for gas

$$\frac{\partial(mu)}{\partial t} + \frac{\partial(\dot{m}h)}{\partial x} dx + \alpha A(T - T_w) + P \frac{dV}{dt} = 0 \quad (1)$$

where  $m$  is mass,  $u$  internal energy,  $\dot{m}$  mass flow rate,  $t$  time,  $h$  enthalpy,  $x$  distance,  $T$  gas temperature,  $T_w$  temperature of solid,  $P$  gas pressure,  $\alpha$  heat transfer coefficient,  $A$  heat transfer area, and  $V$  volume.

Continuity equation for gas flow

$$\frac{\partial m}{\partial t} = \dot{m}_{in} - \dot{m}_{out} \quad (2)$$

where  $\dot{m}_{in}$  is mass flow rate at the inlet and  $\dot{m}_{out}$  mass flow rate at the outlet of a given volume.

Momentum equation for gas flow

$$\frac{\partial P}{\partial x} = -fg \frac{1}{d} \frac{Pv^2}{2} \quad (3)$$

where  $fg$  is coefficient of friction,  $d$  hydraulic diameter, and  $v$  gas velocity.

Energy equation for regenerative materials

$$m \frac{\partial(C_w T_w)}{\partial t} = \alpha A(T - T_w) \quad (4)$$

where  $C_w$  is specific heat of regenerative materials.

Gas state equation

$$h = f(T, P) \quad \text{or} \quad T = f(h, P) \quad (5)$$

where  $f$  is function. The equation (4) can represent ideal gas or real gas.

**MAJOR CONTRIBUTIONS OF NUMERICAL ANALYSIS**

**1. Concept of “Gas Piston” and Function of Phase Shifting in Orifice PT Cryocooler**

A numerical simulation of orifice PT cryocooler was first performed by Wu and Zhu [6] in 1989 at Xian Jiaotong University. It demonstrated the internal working process of an orifice PT cryocooler. It revealed and confirmed a concept of “gas displacer” in the pulse tube where a portion of gas (the gas displacer) never leaves the pulse tube (see Figure 1). The “gas displacer” is a very useful concept for understanding the operation of PT cryocoolers and comparing with traditional cryocoolers.

The gross refrigeration power (time average enthalpy flow in the pulse tube), assuming an ideal gas, is given by

$$\langle \dot{H}_p \rangle = \left(\frac{c_p}{\tau}\right) \int_0^\tau \dot{m} T dt \quad \text{or} \quad \langle \dot{H}_p \rangle = \left(c_p * \frac{A_p}{R\tau}\right) \int_0^\tau p u dt \quad (6)$$

where  $A_p$  is the cross area of the pulse tube,  $R$  gas constant,  $p$  gas pressure, and  $u$  gas velocity.

Figure 2 shows the simulation results for the dynamic pressure and gas velocity in the pulse tube with three orifice openings. The results show a phase-shifting mechanism in the orifice PT cryocooler for optimum cooling performance.

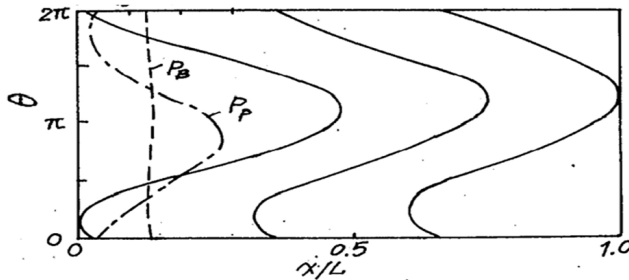


**Figure 1.** Traces of three particales in a cycle.  $\theta$  is angle in a cycle;  $x/L$  is relative position in a pulse tube.

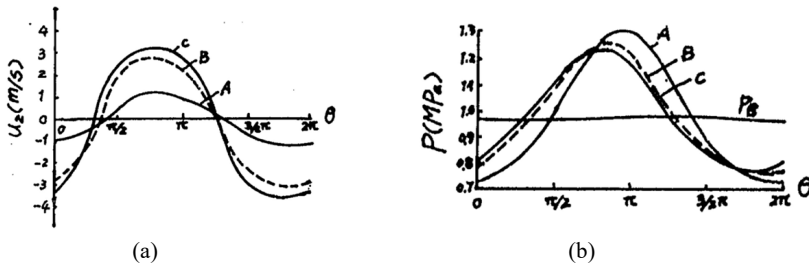


**Figure 2.** Dynamic gas velocity and pressure at the hot end of a pulse tube with three orifice openings. Orifice opening: A:0.0371; B: 0.0643; C:0.0742. (a) dynamic gas velocity; (b) dynamic pressure.

## 2. Invention and Function of the Second Orifice in PT cryocooler

The numerical analysis, performed by Zhu et al in the same group at Xian Jiaotong University, found a larger gas mass flow rate through a regenerator in an orifice PT cryocooler (larger than that in Stirling cryocooler) and a portion of it has no refrigeration effect. A second orifice was proposed for the orifice PT cryocooler and led to an important invention, called “double-inlet PT cryocooler” [7].

Numerical simulation, with a step piston for the second inlet, was performed and showed significant improvement in the PT cryocooler performance. The numerical simulation at that time did not include the momentum equation (flow resistance) and could not analyze the function of the second orifice during the invention since the gas flow through the second orifice is driven by the pressure difference across it.

Later on, a numerical modeling including the momentum equation (flow resistance) was accomplished by Wang et al in the same group to simulate the double-inlet PT cryocooler [8], which revealed phase-shifting mechanisms and efficiency improvement by adding the second orifice in the double-inlet PT cryocooler (see Figure 3).

Table 1. shows variations of cooling capacity and power input with four openings of the second orifice. The second orifice reduces the power input and increases the cooling capacity by obtaining a better phase-shifting for the orifice PT cryocooler.

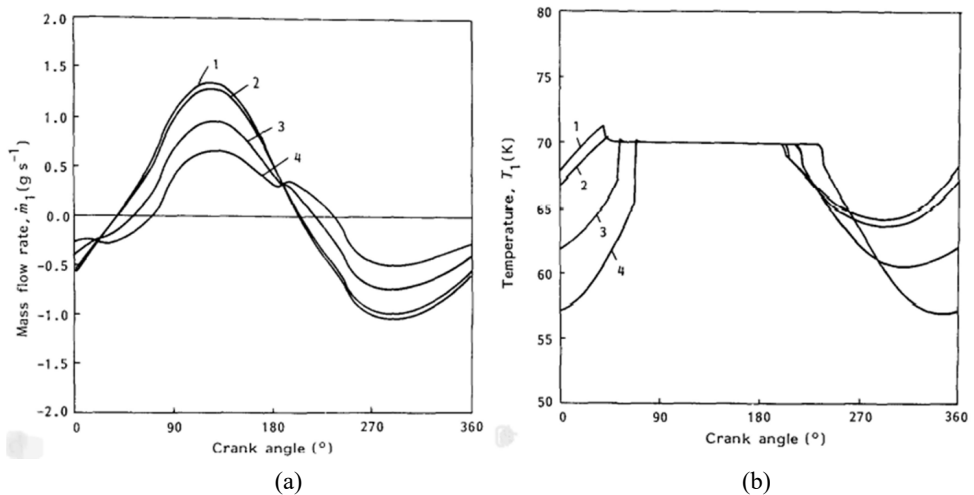


**Figure 3.** Dynamic mass flow rate and dynamic temperature in a cycle at the cold end of the pulse tube. Second orifice opening: 1.  $A=0.0$ ; 2.  $A=0.0314$ ; 3.  $A=0.196$ ; 4.  $A=0.385$ . (a) mass flow rate; (b) temperature.

**Table 1.** Performances of a double-inlet PT cryocooler by numerical simulation

	Calculation 1	Calculation 2	Calculation 3	Calculation 4
$A_v$ (mm <sup>2</sup> )	0	0.0314	0.196	0.385
$Q$ (W)	5.45	5.76	6.77	6.50
$W$ (W)	98.1	96.1	86.6	77.6
$r_c$	1.60	1.61	1.66	1.71
$r_D$	1.34	1.36	1.47	1.59
$\eta$ (%)	5.6	6.0	7.8	8.3

In Table 1,  $A_v$  is the second orifice opening,  $Q$  is cooling capacity,  $W$  is power input,  $r_c$  is the pressure ratio in the compressor,  $r_p$  is the pressure ratio in the pulse tube, and  $\eta$  is efficiency.

**3. Reveal DC gas flow Effect in PT Cryocoolers.**

The second orifice connection in a double-inlet PT cryocooler builds a closed-loop for possible circulation gas flow (so-called DC flow), which is shown in figure 4. Gedeon [9] first analyzed the possible DC flow in a Stirling cryocooler and a double-inlet PT cryocooler using “Sage” software in 1997. The DC gas flows were discovered in numerical simulations and the results indicated the root of the problems are in-phase density and velocity fluctuations in the flow-resistive elements of the closed loop which tend to produce a DC pressure gradient.

Figures 5 (a) and (b) show the large impacts of a small amount of DC flow on the temperature profiles in the regenerator and pulse tube.

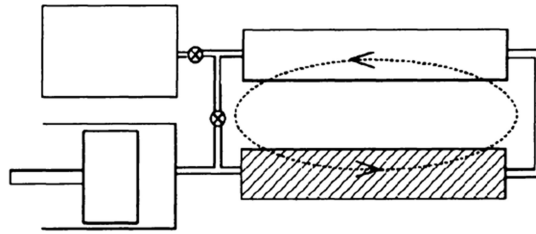


**Figure 4.** Possible DC flow in a double-inlet PT cryocooler

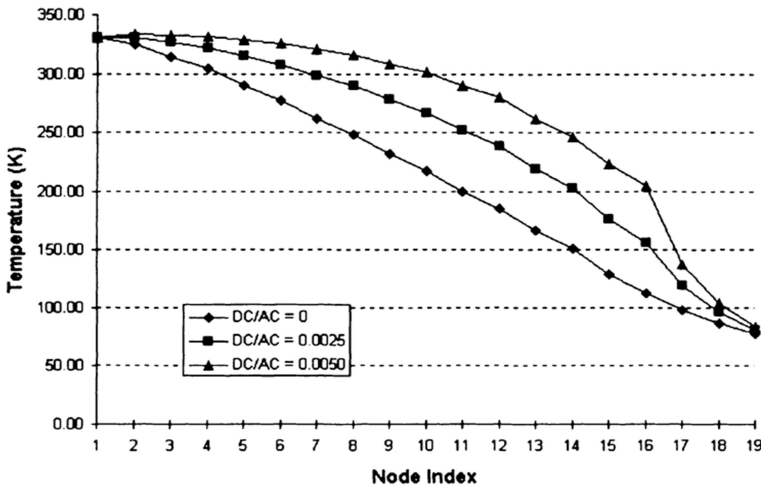


**Figure 5a.** Temperature profiles in regenerator for various values of DC flow as a fraction of the AC flow amplitude. DC/AC is ratio of the DC gas flow and AC oscillating flow.

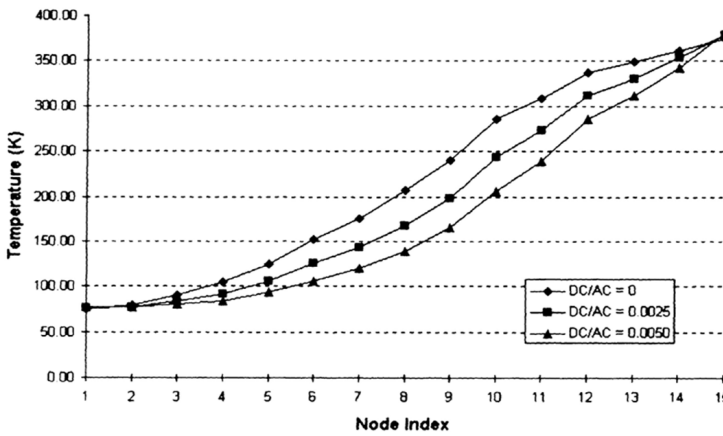


**Figure 5b.** Temperature profiles in pulse tube for various values of DC flow as a fraction of the AC flow amplitude. DC/AC is ratio of the DC gas flow and AC oscillating flow.

Wang et al. performed numerical simulations and experimental tests on DC flow effects in a GM-type single-stage PT cryocooler [10] and a 4 K two-stage PT cryocooler [11]. Numerical analyses help to understand the DC flow effect at different temperature regions. The simulation results in Tables 2 and 3 clearly indicate how the DC flow reduces the cooling performance and impacts energy flow in a single-stage 80 K cryocooler.

The 4 K pulse tube stage has unique features and it performs differently with various values of DC gas flow when compared to a single-stage 80 K cryocooler due to a large intrinsic enthalpy loss. Table 3 shows a small negative DC flow from the hot end of the pulse tube to the inlet of the regenerator improves the cooling performance of the 4 K stage by increasing the enthalpy in the pulse tube and dissipating the hot end gas energy through the double-inlet loop.

#### 4. Reveal Unique Features of 4 K PT Cryocoolers.

Numerical simulation for a 4 K PT cryocooler was first performed by Wang [12,13]. It reveals some unique features of the 4 K regenerator and pulse tube, such as a temperature plateau near the cold end of the regenerator, large temperature swings in the middle of the regenerator,

**Table 2.** Calculated effects of DC flow on the cooler performance in a single-stage PT cryocooler.  $\dot{Q}$ : cooling power;  $\dot{Q}_h$ : heat transfer in hot heat exchanger;  $\dot{H}_r$ ,  $\dot{H}_p$ ,  $\dot{H}_d$ : enthalpy flow through regenerator, pulse tube and double-inlet valve;  $|\dot{m}_h|$ ,  $|\dot{m}_c|$ : time-averaged mass flow rate at the hot and cold end of regenerator.

$\frac{\dot{m}_{DC}}{ \dot{m}_{AC} }$	$\frac{\dot{m}_{DC}}{ \dot{m}_h }$	$\dot{Q}_c$ (W)	$\dot{H}_r$ (W)	$\dot{H}_p$ (W)	$\dot{H}_d$ (W)	$\dot{Q}_h$ (W)
- 11.3 %	-0.0052	11.8	13.8	25.6	-12.1	13.2
- 8.5 %	-0.0038	14.3	10.8	25.1	- 9.3	15.7
- 5.9 %	-0.0026	17.04	15.51	24.8	- 6.4	18.4
-3.3% *	-0.0013	19.2	5.4	24.6	- 3.5	21.1
- 0.61%	-0.00022	19.4	4.8	24.2	- 0.6	23.6
+ 0.47%	+0.00016	19.2	4.7	23.9	+ 0.6	24.5
+ 2.2 %	+0.0007	19.0	4.5	23.5	+ 1.8	25.3
+ 5.2%	+0.0015	18.1	4.2	22.3	+ 4.8	27.1

\* Obtained from the same flow coefficients for two directions of the double-inlet valve.

**Table 3.** Calculated effects of DC flow on the performance of the 4 K cryocooler.  $Q_c$ : cooling power;  $\dot{H}_r$ ,  $\dot{H}_p$ ,  $\dot{H}_d$ : enthalpy flow through regenerator, pulse tube and double-inlet valve;  $\overline{|\dot{m}_h|}$ ,  $\overline{|\dot{m}_c|}$ : time-averaged mass flow rate at the hot and cold end of regenerator.

$\overline{\dot{m}_{DC}} / \overline{ \dot{m}_{AC} }$	$\overline{\dot{m}_{DC}} / \overline{ \dot{m}_i }$	$Q_c$ (W)	$\dot{H}_r$ (W)	$\dot{H}_p$ (W)	$\dot{H}_d$ (W)	$\overline{ \dot{m}_h }$ (g/s)	$\overline{ \dot{m}_c }$ (g/s)
- 2.6 %	-0.0005	0.13	15.50	15.63	- 6.50	7.24	9.46
- 5.2 % *	-0.0010	0.66	15.22	15.88	- 12.03	6.88	9.08
- 7.8 %	-0.0015	1.04	15.51	16.55	- 16.96	6.78	9.00
- 10.4 %	-0.0020	1.27	15.73	17.01	- 21.88	6.64	8.82
- 13.3 %	-0.0026	1.36	16.04	17.40	- 26.81	6.31	8.42

\* Obtained from the same flow coefficients for two directions of the double-inlet valve.

and increased mass flow at the cold end of the regenerator, etc. (see Figures 6 and 7). The numerical simulation helped understand the unique working mechanism and entailed the successful development of the first two-stage 4 K PT cryocooler at Giessen University [14].

Figure 6 shows the temperature profiles of a 4 K regenerator in a cycle. Figure 7 shows dynamic pressures at the cold and warm ends of the regenerator in a cycle. The average mass flow rate at the cold end of the regenerator is larger than that at the warm end. This behavior is different from that in an 80 K regenerator which has a larger mass rate at the warm end.

Intrinsic enthalpy loss of the 2<sup>nd</sup> regenerator in a 4K cryocooler is generated by the real gas property. This portion of enthalpy losses could provide the intercept cooling from the 2<sup>nd</sup> stage regenerator. The intercept cooling has been widely adapted in cryogen-free sub-4K systems, in particular for all continuous flow type systems such as cryogen-free He-3 cryostats and dilution refrigerators where more efficient helium (including He-3) condensation rate is crucial for their performance. It is also used for precooling helium-4 to be liquefied in lab-scale helium liquefiers.

A numerical model had been built for analyzing the effects of the intercept cooling as shown in Figure 8, in which a distributed heat load is applied along with the entire 2<sup>nd</sup> stage regenerator. The numerical simulation, which considers the real gas property, heat transfer, and properties of regenerator materials, was conducted to analyze the impact of the intercept cooling on energy flows in the 4 K stage [15].

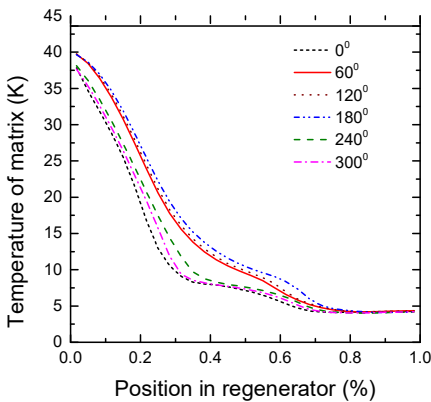


**Figure 6.** Temperature profiles of a 4 K regenerator in a cycle

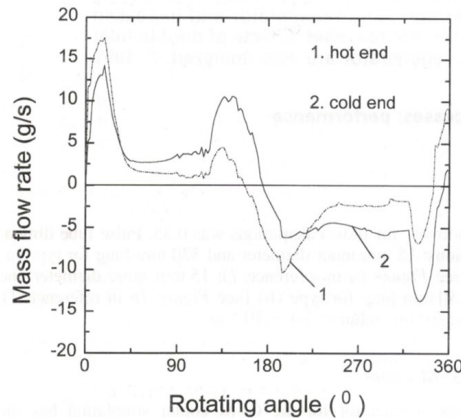


**Figure 7.** Dynamic pressures at the cold and warm ends of the regenerator in a cycle

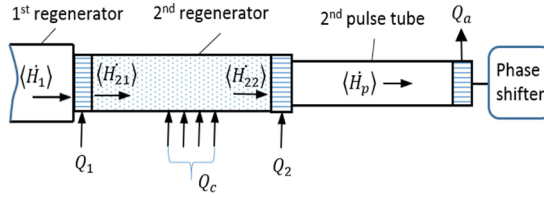


**Figure 8.** Energy flows in the 2<sup>nd</sup> stage of PT cryocooler with a heat load on the regenerator.  $Q_c$  is intercept cooling,  $Q_1$  first stage cooling capacity,  $Q_2$  second stage cooling capacity,  $\langle \dot{H}_1 \rangle$  enthalpy in the first stage regenerator,  $\langle \dot{H}_{21} \rangle$  and  $\langle \dot{H}_{22} \rangle$  enthalpy flows at the two ends of the regenerator.

**Table 4.** Calculated energy flow in the 2<sup>nd</sup> stage of a 4K PT cryocooler

	$\langle \dot{H}_{21} \rangle$ (W)	$\langle \dot{H}_{22} \rangle$ (W)	$\langle \dot{H}_p \rangle$ (W)	$Q_2$ at 4.2K (W)
$Q_c=0$	15.94	15.93	16.54	0.60 (0.57*)
$Q_c=2.0$ 4 W	14.14	16.17	16.54	0.37

\*Experimental data

The numerical simulation results are given in table 4. The applied heat load of 2.04 W total results in slight increase of the enthalpy losses  $\langle \dot{H}_{22} \rangle$  at the cold end of the regenerator by 0.24 W, which is the loss of cooling capacity at 4.2 K. The increased losses might be caused by the real regenerator operation and the higher intercept cooling capacity than the intrinsic enthalpy loss. The enthalpy flow at the inlet of the regenerator  $\langle \dot{H}_{21} \rangle$  is reduced by 1.8 W, which indicates the intrinsic enthalpy loss has been used for the intercept cooling. The intercept cooling reduces the 4 K cooling capacity by ~12% of the intercept cooling load applied on the regenerator. This percentage can vary with different 1<sup>st</sup> stage temperatures and other factors.

## 5. Analysis of New Phase shifters

Numerical simulation has been used to analyze, verify and design a new phase shifter for PT cryocoolers. An active buffer type PT cryocooler was proposed and analyzed with the numerical simulations by Zhu et al [16,17]. The numerical analysis revealed the working mechanism, verified the feasibility of the concept, and optimized the structure parameters for the experimental test.

Figure 9 shows the concept of the active buffer type PT cryocooler. The phase shifter at the warm end of the pulse tube consists of a number of the valves and buffer volumes.

Figure 10 shows the equivalent PV work in the pulse tube with three valve-timings obtained from the numerical simulation. The ideal PV works in the pulse tube can be achieved with proper valve timing.

Figure 11 shows experimental results of the equivalent PV works in the pulse tube of the active buffer type PT cryocooler, which is similar to that obtained from the numerical simulation.

Numerical simulations have been performed on new phase-shifters, such as inductance tube phase-shifter and piston phase-shifter, etc. The numerical analysis performed by Zhu et al. revealed the working mechanism of the inductance tube from the engineering point of view, and assisted researchers to understand and optimize the inductance tube [18,19]. There are more contributions of the numerical simulation in the development of the PT cryocoolers, but this paper is not able to review all of them.



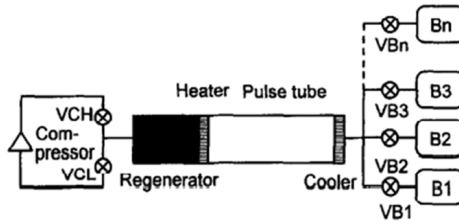


Figure 9. Concept of active buffer PT cryocooler

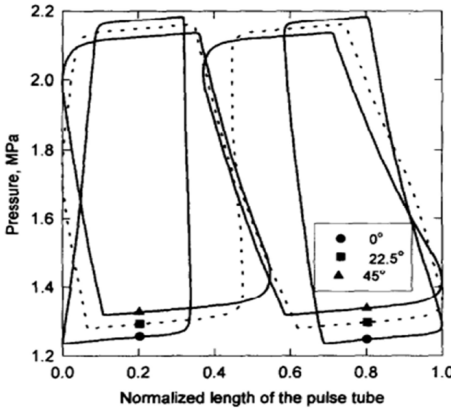


Figure 10. variations of equivalent PV work with three valve timings (from numerical simulation)

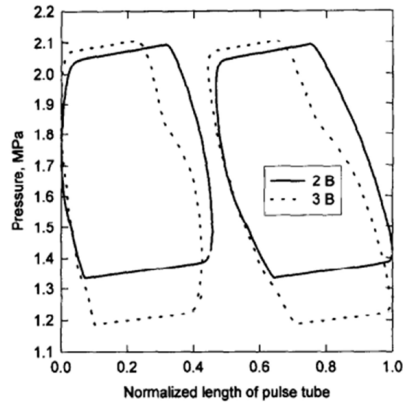


Figure 11. Equivalent PV work with 2 or 3 buffers (from experimental test). 2B, two buffers; 3B, three buffers.

**CONCLUSIONS**

Numerical simulation plays important role in the development of PT cryocoolers by revealing working mechanisms, helping to understand the internal processes and loss mechanisms, optimizing the structure parameters as well as assisting innovations of PT cryocoolers.

**ACKNOWLEDGMENT**

Many thanks to prof. Shaowei Zhu at TongJi University for collecting some references and helpful discussions. Thanks to prof. Limin Qiu at Zhejiang University for providing some references.

**REFERENCES**

1. Gifford, W.E. and Longworth, R.C., "Pulse Tube Refrigeration," *Journal of Engineering for Industry*, 86.3, (1964), pp. 264-268.
2. Mikulin, E.I., Tarasov, A.A. and Shkrebyonock, M.P., "Low-temperature Expansion Pulse Tubes," *Advances in Cryogenic Engineering*, vol. 29, Plenum Press, New York (1984), pp. 629-637.
3. Finkelstein, T., "Computer Analysis of Stirling Engines," *Adv. Cryog. Eng.*, vol.20 (1975), pp.269-282.
4. Walker, G., *Cryocoolers, Part 1*, International Cryogenics Monographs Series, Plenum Press, NY (1983).
5. Tao, W.Q., *Numerical Heat Transfer*, Press of Xian Jiaotong University (1988).

6. Wu, P.Y. and Zhu, S.W., "Mechanism and Numerical Analysis of Orifice Pulse Tube Refrigeration With a Valveless Compressor," *Proceedings of International Conference of Cryogenics and refrigeration*, International Academic Publishers, (1989), pp. 85-90.
7. Zhu, S.W., Wu, P.Y. and Chen, Z.Q., "Double-Inlet Pulse Tube Refrigerators: an Important Improvement," *Cryogenics*, vol. 30, (1990), pp. 514-520.
8. Wang, C., Wu, P.Y. and Chen, Z.Q., "Numerical Analysis of Double-inlet Pulse Tube Refrigerator," *Cryogenics*, vol.33, no. 5 (1993), pp.526-530.
9. Gedeon, D., "DC Gas Flow in Stirling and Pulse Tube Cryocoolers," *Cryocoolers 9*, Plenum Press, New York (1997), p. 385.
10. Wang, C., Thummes, G. and Heiden, C., "Control of DC Gas Flow in a Single-stage Double-inlet Pulse Tube Cooler," *Cryogenics*, vol.38, no. 8 (1998), pp.843-847.
11. Wang, C., Thummes, G. and Heiden, C., "Effects of DC Gas Flow on Performance of Two-stage 4 K Pulse Tube Cooler," *Cryogenics*, vol.38, no. 6 (1998), pp.689-695.
12. Wang, C., "Numerical Analysis of 4 K Pulse Tube Coolers, Part I: Numerical Simulation," *Cryogenics* (1997), Vol.37, No.4, p.207.
13. Wang, C., "Numerical Analysis of 4 K Pulse tube Coolers, Part II: Performances and Internal Processes," *Cryogenics* (1997), Vol.37, No.4, p.215.
14. Wang C., Thummes G. and Heiden C., "A Two-stage Pulse Tube Cooler Operating Below 4K," *Cryogenics*, vol. 37 (1997), p.159.
15. Wang C., "Helium Liquefaction with a 4K Pulse Tube Cryocooler," *Cryogenics*, vol.41 (2001), pp.491-496.
16. Zhu, SW. and Matsubara, Y., "Proposal for a Tube Expander," *Cryogenics*, vol. 36 (1996), pp.403-408.
17. Zhu, S.W., Kakimi, Y and Matsubara, Y., "Investigation of Active-buffer Pulse Tube Refrigerator," *Cryogenics*, vol. 37 (1997), pp.461-471.
18. Zhu SW, Shou SL, Yoshimura N, Matsubara Y., "Phase Shift Effect of the Long Neck Tube for the Pulse Tube Refrigerator," *Cryocooler 9*, New York: Plenum Press (1997), pp.269-278.
19. Zhu SW, Shou SL, Yoshimura N, Matsubara Y., "Numerical Method of Inertance Tube Pulse Tube Refrigerator," *Cryogenics*, vol. 44 (2004), pp.649-660.